Toll-like receptor-5 agonist, entolimod, suppresses metastasis and induces immunity by stimulating an NK-dendritic-CD8$^+$ T-cell axis

Craig M. Brackett[a], Bojidar Kojouharov[a], Jean Veith[a], Kellee F. Greene[a], Lyudmila G. Burdelya[a], Sandra O. Gollnick[a], Scott I. Abrams[b,1], and Andrei V. Gudkov[a,c,1]

[a]Department of Cell Stress Biology, Roswell Park Cancer Institute, Buffalo, NY 14263; [b]Department of Immunology, Roswell Park Cancer Institute, Buffalo, NY 14263; and [c]Cleveland BioLabs, Inc., Buffalo, NY 14203

Edited by Ruslan Medzhitov, Yale University School of Medicine, New Haven, CT, and approved January 5, 2016 (received for review October 28, 2015)

Activation of an anticancer innate immune response is highly desirable because of its inherent ability to generate an adaptive antitumor T-cell response. However, insufficient safety of innate immune modulators limits clinical use to topical applications. Toll-like receptor 5 (TLR5) agonists are favorably positioned as potential systemic immunotherapeutic agents because of unusual tissue specificity of expression, uniquely safe profile of induced cytokines, and antitumor efficacy demonstrated in a number of animal models. Here, we decipher the molecular and cellular events underlying the metastasis suppressive activity of entolimod, a clinical stage TLR5 agonist that activates NF-κB–, AP-1–, and STAT3–driven immunomodulatory signaling pathways specifically within the liver. Used as a single agent in murine colon and mammary metastatic cancer models, entolimod rapidly induces CXCL9 and -10 that support homing of blood-borne CXCR3-expressing NK cells to the liver predominantly through an IFN-γ signaling independent mechanism. NK cell-dependent activation of dendritic cells is followed by stimulation of a CD8$^+$ T-cell response, which exert both antimetastatic effect of entolimod and establishment of tumor-specific and durable immune memory. These results define systemically administered TLR5 agonists as organ-specific immunoadjuvants, enabling efficient antitumor vaccination that does not depend on identification of tumor-specific antigens.

cancer immunotherapy | liver | colorectal cancer | breast cancer | innate immunity

Recent advancements in the field of anticancer immunotherapy have been primarily focused on development of T-cell–based approaches because of recognition of the inherent ability of adaptive immunity to efficiently eradicate neoplastic disease (1, 2). Innate immune responses play important roles in T-cell activation, but their potential relevance for prevention and treatment of cancer remains underappreciated (3–5). Toll-like receptors (TLRs) are gaining attention as potential therapeutic targets capable of stimulating antitumor immunity by initiating innate responses (6) and subsequent adaptive T-cell–based immunity (7). Although proof-of-principle for this concept has been demonstrated with agonists of several TLRs (TLR3, -7, and -9) (8), only one, the TLR7 agonist Imiquimod, has been approved for clinical use [however, this is limited to topical treatment of basal cell carcinoma (9)]. The major clinical limitations of many TLR agonists are the risk of dose-limiting toxicities associated with their systemic delivery (10–12) and metastasis stimulation (13–15). Furthermore, some previously investigated TLR agonists are restricted to injection directly into tumor tissue (3, 16–18), an approach that will likely have limited therapeutic value in cancer patients with metastatic disease.

TLR5 is unique among TLRs as a potential target for systemic anticancer immunotherapy. Studies have shown that the only known natural TLR5 agonist, flagellin, flagellin-expressing *Salmonella* bacteria, and a pharmacologically optimized flagellin derivative named entolimod (CBLB502) have antitumor effects in several tumor models (19–23), including mouse models of liver metastases (24–26). Moreover, systemic administration of TLR5 agonists is uniquely safe because of the restricted pattern of expression of TLR5 (primarily in the gut, liver, and bladder) and the nature of the cytokines induced following TLR5 stimulation. In particular, TLR5 agonists are significantly less toxic than agonists of some other TLRs as a result of the lack of induction of self-amplifying "cytokine storm"-inducing cytokines, such as TNF-α, IL-1β, and IL-2, which can cause septic shock (27–29). Instead, TLR5 agonists induce rapid and short-lived production of high levels of G-CSF, IL-6, IL-8, and IL-10 in all tested species, including rodents, nonhuman primates, and humans (29–31).

The liver shows the strongest TLR5 activation response following systemic entolimod administration characterized by dramatic activation of NF-κB–, STAT3–, and AP-1–driven transcription leading to cytokine production (as described above) and mobilization of different classes of immune cells into the liver (26). In particular, entolimod-driven recruitment of natural killer (NK) cells to the liver was shown to be critical for the antitumor efficacy of the drug in murine tumor models (26, 32) and for its antiviral activity in a mouse model of cytomegalovirus infection (33). The liver is a common site of colorectal cancer (CRC) tumor metastasis (34) and the location of large numbers of NK cells (35), which have been reported to have antitumor activity in the liver (36, 37). NK cells are

Significance

Innate immune modulators can generate a potent antitumor T-cell response and are thus a desirable approach to immunotherapy. However, their use is limited by the risk of induction of acute inflammation. In this regard, bacterial flagellin is unique among other innate immune modulators because of a significantly safer cytokine profile induced upon activation by its target, Toll-like receptor 5 (TLR5). We show here that systemic administration of entolimod, a pharmacologically optimized flagellin derivative, induces a cascade of cell–cell signaling resulting in mobilization to the liver of various components of innate and adaptive immunity, followed by suppression of liver metastases and development of long-term antitumor immune memory. Thus, TLR5 agonists can be considered as an organ-specific immunotherapy for the treatment and prevention of metastases.

Author contributions: C.M.B., L.G.B., S.O.G., S.I.A., and A.V.G. designed research; C.M.B., B.K., J.V., and K.F.G. performed research; C.M.B., L.G.B., S.O.G., S.I.A., and A.V.G. analyzed data; and C.M.B., S.I.A., and A.V.G. wrote the paper.

Conflict of interest statement: A.V.G. and L.G.B. are coinventors of entolimod and, along with C.M.B. and S.O.G., are paid consultants for Cleveland Biolabs, a biotech company that holds the license for clinical use of entolimod and runs its development.

This article is a PNAS Direct Submission.

Freely available online through the PNAS open access option.

[1]To whom correspondence may be addressed. Email: scott.abrams@roswellpark.org or andrei.gudkov@roswellpark.org.

This article contains supporting information online at www.pnas.org/lookup/suppl/doi:10.1073/pnas.1521359113/-/DCSupplemental.

classified as effectors of innate immunity that provide an early host response against viruses, bacteria, and tumors, and play a pivotal role in bridging the innate and adaptive arms of the immune response (38, 39). One mechanism by which NK cells connect innate and adaptive immune responses is through the ability of NK cells to license dendritic cells (DCs), which then stimulate T-cell activation, resulting in development of antigen-specific T-cell–dependent immunity (40–42).

A recent study demonstrated that flagellin up-regulated CXCL10 expression in the cornea and that this contributed to fungal clearance through a CXCR3-dependent NK cell response (43). CXCL9, CXCL10, and CXCL11 are members of the IFN-inducible CXC chemokine family that act through interaction with the CXCR3 (44, 45) receptor found on a variety of cell types, including NK cells (45, 46). Production of chemokines that are CXCR3 ligands leads to chemotactic migration of CXCR3-expressing NK cells to sites of inflammation, infection, and malignancy (47, 48). Levels of CXCL10 are strongly increased (~20-fold) in the plasma of mice after systemic entolimod treatment (29). These findings led us to hypothesize that entolimod treatment might suppress liver metastases and stimulate long-term T-cell–dependent protective antitumor immunity through CXCR3-dependent homing of NK cells to the liver.

Testing of this hypothesis in mouse models of syngeneic CT26 CRC experimental liver metastasis and spontaneous liver and lung metastasis of 4T1 mammary tumors showed that entolimod treatment generates protective $CD8^+$ T-cell–dependent antitumor memory. In the CT26 model, the entolimod-elicited NK cell response was essential for dendritic cell licensing and activation of $CD8^+$ effector T cells in the liver independently of $CD4^+$ T cells. In contrast, we found that antimetastatic activity of entolimod in the spontaneous 4T1 metastatic model was less dependent on NK cells but dependent on both $CD8^+$ and $CD4^+$ T cells. In addition, CXCR3 expressed by NK cells regulates the therapeutic efficacy of entolimod by supporting their blood-borne homing to the liver where entolimod stimulates production of the CXCR3 ligands CXCL9 and -10. Interestingly, whereas entolimod stimulates production of IFN-γ in the liver and CXCL9 and CXCL10 are known to be IFN-γ–regulated (49, 50), expression of CXCL9 and CXCL10 was, at least in part, IFN-γ–independent in this system. These results indicate that entolimod treatment leads to development of systemic T-cell–dependent antimetastatic activity by altering the liver microenvironment. Therefore, pharmacological targeting of TLR5 represents a novel therapeutic strategy for safe and effective treatment of what are currently the most poorly treatable cancer cases.

Methods

Mice. Pathogen-free BALB/cAnNCr and C57BL/6NCr mice were obtained from the National Cancer Institute; C.B-Igh-1blcrTac-Prkdcscid/Ros (SCID) mice were obtained from Laboratory Animal Resources at Roswell Park Cancer Institute (RPCI); C.129S4-*Cxcr3*^{tm1Arsa}/SoghJ (*Cxcr3*$^{-/-}$) and C57BL/6N-*Ifngr1*$^{tm1.2Rds}$/J (*Ifngr1*$^{-/-}$) were bred and maintained by RPCI Laboratory Animal Resources. All mice were female and were housed in microisolator cages in a laminar flow unit under ambient light. The RPCI Institutional Animal Care and Use Committee approved all procedures carried out in this study.

Reagents. The TLR5 agonist entolimod (CBLB502) is a cGMP-manufactured drug product that was obtained from Cleveland BioLabs, Inc. (29).

Cell Lines. Murine colon carcinoma CT26 cells and mammary carcinoma 4T1 cells were obtained from American Type Culture Collection and cultivated in RPMI medium with 10% (vol/vol) FBS, penicillin/streptomycin, and L-glutamine in a humidified chamber at 37 °C with 5% CO_2.

Experimental and Spontaneous Liver Metastasis Models. Experimental liver metastases of CT26 CRC tumors were established via intrasplenic injection of 2×10^5 CT26 tumor cells in 100 μL of PBS followed by splenectomy, as previously described (26, 51). In the 4T1 model, metastasis was evaluated in a clinically relevant set-up following surgical removal of orthotopic 4T1 tumors (26, 52) established by subcutaneous inoculation of 10^5 4T1 cells in 50 μL of PBS into the mammary fat pad. Primary tumors were resected when they reached 200 mm^3 in volume and mice were treated with PBS or entolimod on days 1, 3, and 5 postsurgery. Unless otherwise noted, entolimod (or PBS vehicle control) treatment was subcutaneously with a dose of 1 μg per mouse in a dosing volume of 100 μL PBS.

FACS Staining and Analysis. Single-cell suspensions were obtained from mouse livers by in vivo perfusion with a solution of 0.5 μM EGTA (Sigma-Aldrich) containing 0.2 mg/mL collagenase type IV (Worthington Biochemical) followed by mechanical disruption and in vitro digestion for 30 min at 37 °C. Mouse blood was collected via the submandibular vein into tubes with heparin (10% of final volume) and red blood cells were lysed using a solution of ammonium chloride for 5 min at room temperature. Single-cell suspensions of liver or blood cells were stained for 20 min at 4 °C with the following mixtures of monoclonal antibodies (mAbs): (*i*) APC-efluor780 CD45 (clone 30-F11), Brilliant violet (BV) 785 CD3ε (clone 145-2C11), APC NKp46 (clone 29A1.4), BV510 CD8 (clone 53-6.7), PerCPCy5.5 CD4 (clone RM4-5), FITC CD44 (clone IM7), BV421 CXCR3 (clone CXCR3-173), and PE-Cy7 IFN-γ (clone XMG1.2); and (*ii*) CD45, BV605 CD11c (clone N418), PerCPCy5.5 CD40 (clone 3/23), and PE CD86 (clone GL-1). Anti-NKp46, anti-CD44, anti-CD11c, anti-CD40, and anti-CD86 were purchased from BioLegend; anti-CD45 was from eBioscience; and anti-CD3ε, anti-CD8, anti-CD4, anti-CXCR3, and anti–IFN-γ were from BD Biosciences. After staining, cells were fixed in 2% ultrapure formalin. For intracellular IFN-γ staining, samples were processed in the presence of GolgiStop (BD Biosciences) and staining was performed using FoxP3/Transcription Factor Staining Buffer Set (eBioscience) according to the manufacturer's protocol. Data were acquired on a LSRII Fortessa instrument (Becton Dickinson), stored in Listmode format, and analyzed using WinList software (Verity House Software).

Lymphocyte Depletion in Mice. BALB/c mice were injected intraperitoneally with mAbs against CD8 (clone 53-6.7; BioXcell) or CD4 (clone GK1.5; BioXcell) at a dose of 400 μg per injection or asialo GM1 (Wako Chemicals) at a dose of 50 μg per injection to establish and maintain CD8, CD4, or NK cell depletion, respectively, during the treatment period as previously described (53). Appropriate isotype controls (BioXcell) were injected using the same dose and regimen as the depletion Abs. Depletion was confirmed by FACS analysis of blood samples collected 2 d after Ab injections.

Competitive Short-Term NK Cell Homing Assay. Naïve NK cells were purified from the spleens of BALB/c or *Cxcr3*$^{-/-}$ mice using negative isolation kits purchased from Miltenyi Biotec; purity was confirmed by FACS analysis and was routinely greater than 95%. BALB/c NK cells were labeled with Vybrant CFDA SE Cell Tracer Kit (Invitrogen) and *Cxcr3*$^{-/-}$ NK cells were labeled with CellTracker Orange CMTMR (CTO; Molecular Probes). An equal ratio of BALB/c to *Cxcr3*$^{-/-}$ NK cells (10^6 cells of each genotype) was adoptively transferred intravenously into mice 2.5 h after entolimod or PBS treatment. Livers were harvested 2 h later by in vivo perfusion followed by in vitro digestion as described above to assess presence of adoptively transferred BALB/c and *Cxcr3*$^{-/-}$ NK cells by FACS analysis.

Measurement of Chemokine Levels. Livers and EDTA-treated blood were collected at the indicated time points posttreatment. Centrifugation was used to obtain plasma from EDTA-treated blood. Livers were flash-frozen on dry ice to generate total protein lysates as previously described (26). Briefly, frozen liver tissue was pulverized into a powder and then lysed with RIPA buffer containing protease inhibitor mixture (Sigma). Cellular debris was removed by centrifugation. Total protein concentrations were determined using the Bio-Rad Protein Assay. ELISA kits specific for murine IFN-γ, CXCL9, CXCL10, and CXCL11 were purchased from R&D Systems and used according to the manufacturer's instructions. Results obtained from liver lysates and plasma were normalized per microgram of total protein or per ml plasma, respectively.

T-Cell Studies in SCID Mice. Naïve $CD8^+$ or $CD4^+$ T cells were purified from the spleens of BALB/c mice using negative isolation kits purchased from Miltenyi Biotec. The purity of the obtained cells was confirmed by FACS analysis and was routinely greater than 95%. One day (for survival studies) or 5 d (for FACS studies) after intrasplenic inoculation of CT26 tumor cells, T cells were adoptively transferred into SCID mice by intravenous injection in a volume of 200 μL. NK cell depletion antibodies (anti-asialo GM1, given at 50 μg in a volume of 200 μL per injection) were administered intraperionteally the day of CT26 inoculation (d0) and again on days 1, 7, and 14 (for survival studies) or days 4, 5, and 11 after CT26 inoculation (for FACS studies); rabbit IgG isotype controls were injected using the same dose and regimen. Entolimod was administered on days 2 and 3 for survival studies and days 5 and 6 for FACS studies.

Assessment of T-Cell Memory. BALB/c mice that remained free of CT26 liver tumors or 4T1 metastases for more than 100 d from the time of CT26 inoculation or 4T1 surgery, respectively, were considered cured. To test for the presence of T-cell–dependent antitumor memory in mice cured of CT26 metastases by entolimod treatment, the cured mice were depleted of $CD8^+$ or $CD4^+$ T cells using mAbs, as described above, and then challenged subcutaneously with 2×10^5 CT26 tumor cells. Depletion was confirmed by FACS analysis of blood samples collected 2 d after Ab injections. Growth of subcutaneous tumors was monitored by measurement with a digital caliper. For mice cured of 4T1 metastases by entolimod treatment, splenic T cells from 4T1-cured or naïve mice were expanded in vitro with anti-CD3/anti-CD28 dynabeads (Invitrogen) + plate-bound anti-41BB (clone 3H3; 10 μg/mL; BioXcell) for 4 d followed by Miltenyi negative purification of either $CD8^+$ or $CD4^+$ T cells; purity was routinely greater than 95%. These cells were then transferred intravenously into BALB/c mice inoculated intravenously with either 4T1 (5×10^4) or CT26 (2×10^5) tumor cells 3 d prior (1×10^6 each of $CD8^+$ and/or $CD4^+$ T cells per mouse). Mice were killed on day 30 after tumor cell injection and lungs were harvested to quantify the number of lung tumors under a dissecting microscope.

Antibody-Mediated Depletion of IFN-γ. Mice were injected intraperitoneally with purified anti-mouse IFN-γ (clone XMG1.2) or an appropriate isotype control (both purchased from BioXcell) at a dose of 250 μg 24 h and 30 min before subcutaneous injection of entolimod, as previously described (54). Livers and blood were collected at the indicated times after entolimod injection for assessing expression of CXCL9 and CXCL10 by ELISA, as described above.

Tumor Growth Measurements. Orthogonal diameters of tumors were measured every other day with digital calipers. Tumor volume, V, was calculated using the formula $V = (lw^2/2)$, where l is the longest axis of the tumor and w is the axis perpendicular to l. Tumors were monitored until they reached a volume greater than 400 mm^3, at which time the mice were killed. Animals were considered cured if they had no detectable tumor for more than 100 d.

Statistical Evaluation. All measured values are presented as mean ± SEM. Nonpaired Student's t tests were used for comparisons between groups in all experiments except for survival experiments, which were analyzed by log-rank test. In all cases, statistical significance was defined as $P < 0.05$.

Results

Entolimod Suppresses CRC Liver Metastasis and Generates $CD8^+$ T-Cell Immunity Through NK Cell-Dependent DC Activation. Entolimod treatment of mice bearing experimental CT26 CRC liver metastases increased the proportion of animals that remained tumor free for at least 60 d (26). Here, we investigated the role of T cells in the antitumor activity of entolimod by using Abs to deplete $CD8^+$, $CD4^+$, or both $CD8^+$ and $CD4^+$ T cells before entolimod treatment in mice given experimental CT26 liver metastases. As expected, treatment with entolimod (and rat IgG control Ab) led to a significant increase in animal survival time indicative of reduced CT26 metastasis (Fig. 1*A*). This survival benefit of entolimod was eliminated by depletion of $CD8^+$ T cells, but was not affected by depletion of $CD4^+$ T cells.

We previously reported that the entolimod-elicited NK cell response within the liver is important for the antimetastatic activity of the drug (26). Because NK cells promote T-cell activation (55), we hypothesized that generation of $CD8^+$ T-cell–dependent tumor immunity by entolimod is regulated by NK cells. To test this hypothesis, we used a two-pronged approach that included: (*i*) antibody-mediated cell depletion in BALB/c mice, and (*ii*) naïve T-cell reconstitution of NK cell-sufficient (rabbit IgG-treated) or NK cell-depleted (anti-asialo GM1-treated) SCID mice. Depletion of NK cells eliminated the antitumor activity of entolimod in BALB/c mice given CT26 liver metastases (Fig. 1*B*), a finding consistent with our previous work (26). In NK cell-depleted BALB/c (Fig. 1*B*) or SCID mice (Fig. 1*C*), the presence or absence of $CD8^+$ T cells had no effect on survival, indicating that interaction between NK and $CD8^+$ T cells is important for the metastasis-suppressive effects of entolimod. Moreover, adoptive transfer of naïve $CD8^+$ T cells into NK cell-sufficient SCID mice followed by entolimod treatment restored the antimetastatic activity of the drug, indicating that the response does not involve $CD4^+$ T cells.

Natural killer T (NKT) cells are liver resident cells that respond to entolimod (26) and can activate antitumor immunity (56). We therefore assessed the response of NKT cells in the CT26 tumor-bearing liver 24 h post-entolimod and whether anti-asialo GM1 antibodies depleted NKT cells. In contrast to the response in naïve livers (26), entolimod had no effect on the NKT cell response in CT26 tumor-bearing livers (Fig. S1), a finding consistent with our recent work in the liver metastatic uveal melanoma model (32). Administration of anti-asialo GM1 antibodies significantly reduced the number of NKT cells in the liver. NKT cells likely play a very minor role in the antimetastatic activity of entolimod, which is supported by the data in Fig. 1*C*, showing that adoptive transfer of $CD8^+$ T cells into SCID mice, which lack NKT cells (57), recapitulated the antimetastatic activity of entolimod in BALB/c mice.

Entolimod treatment of SCID mice reconstituted with naïve $CD8^+$ T cells led to an increase in the absolute number of total NK cells in the blood stream on day 7 after treatment (determined by FACS analysis) (Fig. S2*A*). The proportion of NK cells that were activated ($CD69^+$) in the blood increased by day 7 post-entolimod and remained significantly elevated for at least 21 d posttreatment. In addition, entolimod activated $CD8^+$ T cells in the blood of $CD8^+$ T-cell–reconstituted SCID mice via an NK cell-dependent mechanism (Fig. S2*B*).

To directly demonstrate that NK cells stimulate a $CD8^+$ T-cell response in entolimod-treated mice independent of $CD4^+$ T cells, T-cell activation was measured by FACS analysis on livers from NK cell-sufficient (rabbit IgG-treated) or -depleted (anti-asialo GM1-treated) SCID mice that were inoculated intrasplenicaly with CT26 cells and, 5 d later, given adoptive transfer of naïve splenic T cells (both $CD8^+$ and $CD4^+$ T cells) and entolimod injection (Fig. 1*D*). The number of effector $CD8^+$ T cells (Fig. 1*D*, *Left*) and IFN-γ producers (Fig. 1*D*, *Right*) in the liver on day 10 after entolimod treatment was significantly diminished in NK cell-depleted mice compared with NK cell-sufficient mice. $CD4^+$ T cells were unable to compensate for the generation of an effector $CD8^+$ T-cell response in NK cell-depleted mice. This was not because of absence of a $CD4^+$ T-cell response since NK cell depletion had no effect on $CD4^+$ T-cell effector numbers in the liver following entolimod treatment. However, NK cell depletion did significantly reduce the proportion of IFN-γ–producing effector $CD4^+$ T cells.

NK cells can promote DC activation and augment their ability to stimulate naïve T-cell activation (reviewed in ref. 55). This, together with our finding that NK cells are key mediators of entolimod-induced $CD8^+$ T-cell activation, led us to test whether NK cells promote $CD8^+$ T-cell activation through DC activation in the liver after entolimod treatment. Mice were inoculated intrasplenically with CT26 cells, treated with anti-asialo GM1 to deplete NK cells (or rabbit IgG as a control), and then treated with entolimod (or left untreated, shown as "0 h"). FACS analysis of total liver cells showed that entolimod treatment stimulated an increase in the absolute number of total $CD11c^+$ DCs in the liver, independent of the presence/absence of NK cells (Fig. 1*E*, *Left*). Entolimod treatment also resulted in an increase in the frequency of activated (CD40-expressing) DCs in the livers of NK cell-sufficient mice (Fig. 1*E*, *Right*), but this effect was significantly diminished by NK cell depletion. Similarly, the increases in $CD86^+$ activated DC frequency in the liver and CD86 expression level (mean fluorescence intensity, MFI) observed upon entolimod treatment of NK cell-sufficient mice were almost completely absent in NK cell-depleted mice (Fig. S3).

Mice given experimental CT26 metastases via intrasplenic tumor cell inoculation/splenectomy that survived for at least 100 d after entolimod treatment were considered "entolimod-cured" and were assessed for anti-CT26 immune memory by rechallenging them with a subcutaneous inoculation of CT26 tumor cells. Entolimod-cured mice effectively resisted tumor

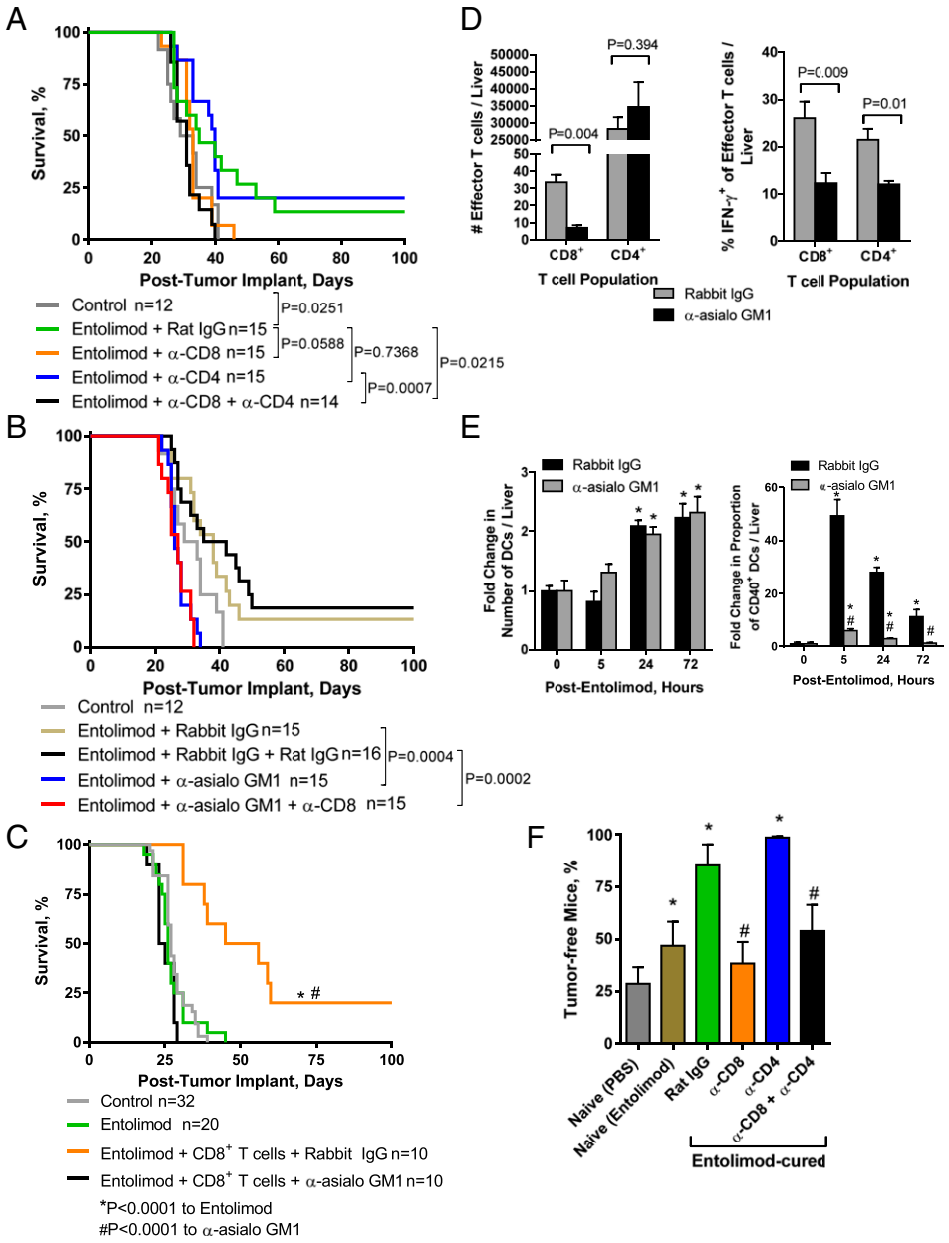

Fig. 1. Entolimod-induced $CD8^+$ T-cell immunity is mediated by NK cell-dependent DC activation. (*A* and *B*) Effect of T-cell and NK cell depletion on survival of entolimod-treated mice following intrasplenic CT26 tumor cell inoculation/splenectomy. (*A*) Mice were treated with anti-CD8 or anti-CD4 depletion antibodies or control rat IgG on days 4 and 11 postinoculation in combination with entolimod given on days 5 and 6. (*B*) Mice were treated with anti-asialo GM1 (on days 4, 5, and 11 postinoculation) or anti-CD8 depletion antibodies (on days 4 and 11 postinoculation) or appropriate control antibodies (rabbit or rat IgG) in combination with entolimod given on days 5 and 6. In all instances, control mice were treated with PBS on days 5 and 6 postinoculation (no Ab treatment). *P* values were determined by log-rank test. (*C*) Effect of NK cell depletion on entolimod-mediated metastasis suppression in T-cell–reconstituted SCID mice. Mice were treated intraperitoneally with anti-asialo GM1 or rabbit IgG on days 0, 1, and 7 after CT26 intrasplenic inoculation and received adoptive transfer of purified naïve BALB/c splenic $CD8^+$ T cells (1.5×10^6 per mouse) on day 1 and entolimod on days 2 and 3. *P* values were determined by log-rank test. (*D*) Effect of NK cell depletion on the absolute number of $CD8^+$ and $CD4^+$ T effector cells and proportion of IFN-γ^+ cells in the livers of T-cell–reconstituted SCID mice. Mice were treated intraperitoneally with anti-asialo GM1 or rabbit IgG on days 4, 5, and 11 after CT26 intrasplenic inoculation and received entolimod followed 2 h later by adoptive transfer of purified naïve BALB/c splenic $CD8^+$ and $CD4^+$ T cells (5×10^6 of each per mouse) on day 5. Total liver cells were isolated on day 10 after entolimod treatment and stained for FACS analysis for effector T cells ($CD45^+CD3\varepsilon^+CD8^+$ or $CD4^+$ and $CD44^{hi}$) and activated effectors (IFN-γ^+). Mean ± SEM; $n = 5$ mice per group. *P* values were determined by Student's *t* test. (*E*) Fold-change in the absolute number of total DCs and proportion of $CD40^+$ DCs in the livers of NK cell-sufficient (rabbit IgG) or -depleted (anti-asialo GM1) entolimod-treated BALB/c mice relative to untreated (0 h) mice. Mice were treated with anti-asialo GM1 or rabbit IgG antibodies (on days 4 and 5 after intrasplenic CT26 inoculation) in combination with entolimod given on days 5 and 6. Total liver cells isolated at the indicated times after entolimod treatment were stained for FACS. DCs were defined as $CD45^+CD11c^+$ and activated DCs were defined by percentage of $CD40^+$ among total DCs. Mean ± SEM; $n = 5$ mice per group. *P* values were determined by Student's *t* test. $^*P < 0.01$ for comparison with 0 h, $^\#P < 0.005$ for comparison with rabbit IgG. (*F*) Effect of T-cell depletion on entolimod-induced immune memory against CT26 tumors. BALB/c mice that survived for >100 d after intrasplenic CT26 inoculation with entolimod treatment ("Entolimod-cured") were depleted of $CD8^+$ and/or $CD4^+$ T cells or mock depleted with rat IgG. One week later, the mice were rechallenged subcutaneously with CT26 tumor cells and the percentage remaining free of subcutaneous tumors for at least 100 d was determined. "Naïve (PBS)" and "naïve (Entolimod)" mice were age-matched animals that were treated with PBS or entolimod, respectively, on days 5 and 6 after splenectomy without intrasplenic CT26 inoculation. After 100 d, these mice were injected subcutaneously with CT26 cells and monitored as described above. Mean ± SEM; $n = 10$ mice per group. *P* values were determined by log-rank test. $^*P < 0.02$ to Naïve, $^\#P < 0.05$ to entolimod-cured + rat IgG.

rechallenge compared with age-matched naïve PBS– or entolimod-treated mice that had not been previously exposed to CT26 cells (Fig. 1*F*), increasing the percentage of mice surviving to day 100 after rechallenge from 29% or 47%, respectively, to 86%. Age-matched naïve mice treated with entolimod showed significant tumor control compared with PBS-treated mice, indicating that entolimod has a general effect on immune responses. To assess the importance of $CD8^+$ and $CD4^+$ T cells for the observed immune memory response against CT26, groups of entolimod-cured mice were antibody-depleted of $CD8^+$ and $CD4^+$ T cells before CT26 rechallenge. Depletion of $CD8^+$ T cells alone or both $CD8^+$ and $CD4^+$ T cells had similar effects, significantly reducing the ability of entolimod-cured mice to resist tumor rechallenge (Fig. 1*F*). In contrast, depletion of only $CD4^+$ T cells did not cause any diminishment in anti-CT26 immunity upon rechallenge of entolimod-cured mice. Taken together, these results show that entolimod stimulates a $CD8^+$ T-cell response capable of suppressing CRC liver metastasis through NK cell-dependent activation of DCs. Moreover, the entolimod-elicited immune response includes formation of durable $CD8^+$ T-cell memory sufficient for protection against tumor cell rechallenge.

The Therapeutic Efficacy of Entolimod Is Regulated by CXCR3-Dependent Blood-Borne Homing of NK Cells to the Liver. Given that NK cells are essential for the antimetastatic activity of entolimod, we next sought to determine the mechanism of entolimod-elicited NK cell accumulation in the liver. Entolimod induces a 20-fold increase in the plasma of the CXCR3 ligand CXCL10 (29). Further characterization of the expression of CXCR3 binding chemokines post-entolimod identified that both CXCL9 and -10 were induced in the liver and plasma of BALB/c mice; however, CXCL11 was not induced by entolimod (Fig. S4). This provided the foundation for the hypothesis that entolimod-elicited CXCL9 and CXCL10 production supports the homing of CXCR3-expressing NK cells to the liver. Entolimod treatment resulted in an increase in the total number of NK cells in the livers of BALB/c mice, but not CXCR3-deficient mice (Fig. 2*A*). To directly test whether CXCR3 supports migration of blood-borne NK cells to the liver after entolimod treatment, we performed a competitive homing assay in which naïve NK cells purified from the spleens of BALB/c or *Cxcr3*$^{-/-}$ mice were labeled with different fluorescent dyes (see *Methods*) and transferred intravenously into mice 2.5 h after entolimod or PBS treatment. FACS analysis of livers isolated 4.5 h after entolimod treatment showed that entolimod stimulated homing of BALB/c NK cells to the liver to a much greater extent than *Cxcr3*$^{-/-}$ NK cells (Fig. 2*B*). The ratio of BALB/c to *Cxcr3*$^{-/-}$ NK cells in the liver increased significantly from 1.4 in control PBS-treated mice to 5.3 in entolimod-treated mice.

The absence of an NK cell response in CXCR3-deficient mice post-entolimod led us to assess the efficacy of entolimod against CT26 metastasis (using animal survival as a readout) in mice globally deficient for CXCR3 (*Cxcr3*$^{-/-}$) versus BALB/c mice. The survival benefit provided by entolimod in this experimental system to wild-type mice was completely absent in *Cxcr3*$^{-/-}$ mice (Fig. 2*C*). Moreover, survival time was significantly shorter for control (no entolimod treatment) *Cxcr3*$^{-/-}$ mice bearing experimental CT26 liver metastases than for corresponding control BALB/c mice, indicating more rapid development of liver metastases due to absence of CXCR3-dependent tumor immunosurveillance.

Given that entolimod promotes NK cell-dependent DC activation and that the NK cell response is abrogated in *Cxcr3*$^{-/-}$ mice, we next evaluated the DC response to entolimod in *Cxcr3*$^{-/-}$ mice versus BALB/c mice by quantifying the DC content of livers by FACS. The number of total $CD11c^+$ DCs in the liver after entolimod treatment was similar between BALB/c and *Cxcr3*$^{-/-}$ mice, except at 5 h posttreatment (Fig. 2*D*, *Left*). However, the frequency of CD40-expressing DCs (Fig. 2*D*, *Right*) and CD86-expressing DCs and CD86 intensity (MFI) (Fig. S5) were significantly lower in entolimod-treated *Cxcr3*$^{-/-}$ mice than in BALB/c mice. These results indicate that the role of NK cells in DC activation following entolimod treatment is fully dependent on CXCR3.

Expression of CXCL9 and CXCL10 is IFN-γ–regulated (49, 50). Entolimod stimulated production of IFN-γ in the livers of mice 2 h posttreatment (Fig. 3*A*). We therefore sought to understand whether entolimod treatment up-regulates CXCL9 and CXCL10 expression downstream of IFN-γ production, thereby providing the signal leading to recruitment of CXCR3-expressing NK cells to the liver. To test this hypothesis, expression of CXCL9 and CXCL10 and NK cell recruitment to the liver in response to entolimod treatment was assessed by antibody-mediated depletion of IFN-γ, which effectively eliminated IFN-γ in the liver (Fig. S6) and IFN-γ receptor-deficient (*Ifngr1*$^{-/-}$) mice. Depletion of IFN-γ only had a significant impact on CXCL10 plasma levels, showing a 50% reduction at both 2 and 5 h post-entolimod (Fig. 3*B*). NK cell recruitment to the liver by entolimod was not significantly affected ($P = 0.1001$) in IFN-γ–depleted mice (Fig. 3*C*). Mice lacking the IFN-γ receptor showed a 50% reduction in entolimod-elicited plasma levels of CXCL9 but not CXCL10 5 h posttreatment (Fig. S7*A*). NK cell recruitment to the livers of these mice 5 h post-entolimod was partially dependent upon IFN-γ receptor signaling, showing a fivefold increase in wild-type mice and a fourfold increase in *Ifngr1*$^{-/-}$ mice (Fig. S7*B*).

Collectively, these data provide support for a mechanism of entolimod's antimetastasis activity that relies upon CXCR3-dependent, predominantly IFN-γ or IFN-γ signaling independent, homing of NK cells to the liver where they stimulate $CD8^+$ T-cell responses through activation of DCs.

CXCR3 Regulates Antimetastatic Activity of Entolimod Against Spontaneous Metastatic Mammary Cancer. To extend our findings to another model of tumor metastasis, we used the 4T1 mammary tumor model in which tumors spontaneously metastasize to the liver and lungs following surgical removal of primary tumors growing orthotopically in the mammary fat pad. Our previous work (26) in this model demonstrated that entolimod significantly extended long-term survival, which despite the presence of disseminated liver metastases, is primarily a reflection of lung metastases (52). Therefore, the survival benefit provided by entolimod in the 4T1 model suggests that the drug may be efficacious against both liver and lung metastases. To examine whether this involves a CXCR3-dependent mechanism, we compared survival of BALB/c versus *Cxcr3*$^{-/-}$ mice after surgical removal of primary orthotopic 4T1 tumors and treatment with PBS or entolimod on days 1, 3, and 5 postsurgery. Consistent with our previous work (26), entolimod treatment significantly prolonged long-term survival of wild-type mice, indicating suppression of tumor metastases (Fig. 4*A*). However, this effect was completely absent in identically treated 4T1-bearing *Cxcr3*$^{-/-}$ mice. Notably, as in the experimental CT26 liver metastasis model, survival was significantly diminished in control (PBS-treated) *Cxcr3*$^{-/-}$ mice compared with control wild-type mice, indicating that CXCR3 is also important for immunosurveillance independent of entolimod. Upon necropsy at the time of death, mortality in this experiment was confirmed to be a result of significant lung metastases.

We assessed the contribution of NK, $CD8^+$, and $CD4^+$ T cells to the antimetastatic activity of entolimod using antibody-mediated cellular depletion after surgical removal of primary 4T1 tumors. Although depletion of NK cells with anti-asialo GM1 diminished the survival benefit provided by entolimod (Fig. 4*B*), this difference was not statistically significant ($P = 0.2187$). In contrast, depletion of either $CD8^+$ or $CD4^+$ T cells significantly reduced survival to the same extent as simultaneous depletion of all three cell types (NK, $CD8^+$, and $CD4^+$ T cells). Depletion of $CD4^+$ T cells had a slightly greater negative effect on entolimod-mediated survival compared with depletion of NK or $CD8^+$ T cells. Although administration of rabbit IgG antibodies appeared

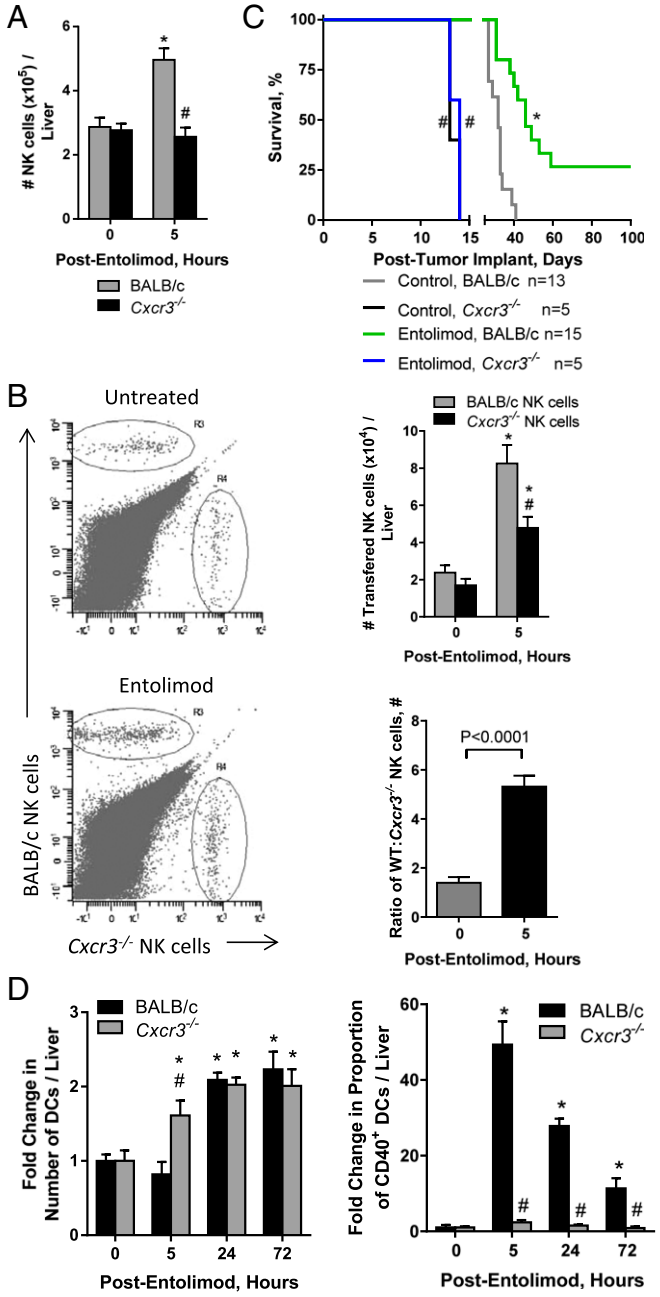

Fig. 2. Entolimod stimulates CXCR3-dependent homing of NK cells to the liver. (*A* and *B*) Mice were injected (subcutaneously) with PBS (untreated) or entolimod on day 5 after intrasplenic CT26 tumor cell inoculation. Data are represented as mean ± SEM. *P* values were determined by Student's *t* test. (*A*) Absolute number of total NK cells in the livers of CT26-inoculated PBS- or entolimod-treated BALB/c or *Cxcr3*$^{-/-}$ mice. FACS analysis for NK cells was performed on total liver cells isolated 0 h (untreated) or 5 h after entolimod treatment using mAb against CD45, CD3ε, and NKp46. Results are reported as the absolute number of NK cells per liver. $n = 8$–23 mice per group; $^{*}P = 0.0007$ for comparison with control, $^{\#}P = 0.0008$ for comparison with 5-h BALB/c. (*B*) Competitive homing assay demonstrating that entolimod-induced homing of NK cells to the liver is CXCR3-dependent. Purified splenic NK cells from BALB/c or CXCR3-deficient mice were labeled with CFDA or CellTracker orange, respectively, and adoptively transferred (in an equal ratio) into PBS- or entolimod-treated BALB/c mice, as described in *Methods*. Livers were collected 4.5 h after treatment for FACS analysis. NK cells of the different genotypes were detected based on the fluorescent cell label in combination with CD45, CD3ε, and NKp46 markers (using mAbs). $n = 5$ mice per group; $^{*}P < 0.02$ for comparison with control, $^{\#}P = 0.01$ for comparison with 5-h BALB/c NK cells. (*C*) Kinetics of mortality for BALB/c or *Cxcr3*$^{-/-}$ mice that were injected (subcutaneously) with PBS (control) or entolimod on days 5 and 6 after intrasplenic CT26 tumor cell inoculation. *P* values were determined by Log-rank test. $^{*}P = 0.0001$ for comparison with control, $^{\#}P < 0.01$ for comparison with BALB/c. (*D*) Fold-change in the absolute number of total DCs defined by CD45^{+}CD11c^{+} and proportion of CD40^{+} DCs in the livers of BALB/c or *Cxcr3*$^{-/-}$ treated with entolimod or PBS (0h). Total liver cells were isolated at the indicated times after entolimod/PBS treatment and stained for FACS with a mixture of mAbs against CD45, CD11c, and CD40. $n = 5$ mice per group; $^{*}P < 0.03$ for comparison with control, $^{\#}P < 0.01$ for comparison with BALB/c.

to reduce the antimetastatic activity of entolimod, this was not significantly different ($P > 0.1691$) from entolimod-treated mice given either rat IgG or a combination of rabbit and rat IgG. This finding suggests that unlike in the CT26 experimental liver metastatic model, CD4^{+} T cells are required for entolimod-elicited generation of antitumor immunity against spontaneous mammary cancer metastases.

To determine whether the antitumor mechanisms induced by entolimod could provide protective immune memory against 4T1 tumors, mice that survived for at least 100 d after primary tumor removal in the experiment shown in Fig. 4*A* were rechallenged with a subcutaneous injection of 4T1 cells in the opposite mammary fat pad (without any further treatment). Naïve mice (100%) developed 4T1 tumors in the fat pad within 16 d of inoculation, compared with only 45% of mice previously "cured" by entolimod treatment (Fig. 4*C*). Additionally, these mice remained free of detectable tumors for at least 100 d following subcutaneous 4T1 rechallange. Importantly, although there were a small number of control vehicle-treated mice that did not develop 4T1 metastases after the original inoculation/surgery (Fig. 4*A*), these animals did not display protective immunity against 4T1 rechallenge (100% developed tumors by day 21 after rechallenge).

We next used an adoptive T-cell transfer approach to assess the effector memory response of T cells from "4T1-cured" mice (survivors from the rechallenge in Fig. 4*C*) against lung tumors established via intravenous injection of 4T1 tumor cells, as previously described (58). Following in vitro expansion and purification, CD8^{+}, CD4^{+}, or CD8^{+} and CD4^{+} T cells from naïve or 4T1-cured mice were adoptively transferred into BALB/c mice 3 d after establishing 4T1 lung tumors. Naïve T cells (CD8^{+}, CD4^{+}, or CD8^{+} and CD4^{+}) did not provide any significant antitumor benefit to these mice (Fig. 4*D*, *Left*). In contrast, transfer of CD8^{+} T cells from 4T1-cured mice resulted in effective control of 4T1 lung tumor development. CD4^{+} T cells from 4T1-cured mice did not provide protection against 4T1 tumors and the effect of CD4^{+} plus CD8^{+} T cells was no greater than that of CD8^{+} T cells alone. The tumor-specificity of the effector memory response was tested in a second cohort of mice injected intravenously with CT26 tumor cells, which leads to development of lung tumors. Both CD8^{+} and CD4^{+} T cells from 4T1-cured mice suppressed development of CT26 lung tumors when transferred separately (Fig. 4*D*, *Right*). However, these effects were considerably weaker than what was observed against 4T1 tumors with transfer of 4T1-cured CD8^{+} or CD4^{+} and CD8^{+} T cells, indicating tumor-type specificity of the generated memory immune response.

Overall, these data indicates that the antimetastatic activity of entolimod is not limited to a particular tumor model or to liver-metastasizing cancers, but is also relevant to lung metastasizing cancers. The mechanism underlying entolimod-mediated suppression of 4T1 mammary tumor metastasis to the lung was found to be similar to that involved in suppression of CT26 CRC tumor metastasis to the liver in that CXCR3 is required along with T cells. However, in contrast to the CT26 model, metastasis suppression in the 4T1 model did not absolutely depend upon NK cells, and in addition to CD8^{+} T cells, CD4^{+} T cells were also important. Tumor type-specific immune memory generated in entolimod-treated mice was primarily mediated by CD8^{+} T cells.

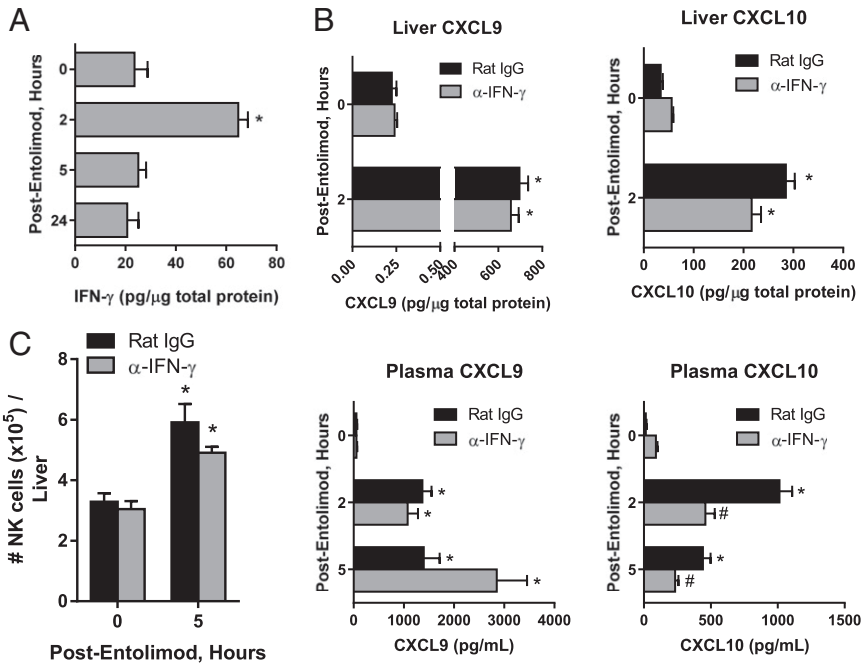

Fig. 3. Entolimod stimulates expression of CXCL9 and CXCL10 and NK cell recruitment to the liver independently of IFN-γ. (*A*) Effect of entolimod treatment on expression of IFN-γ in the mouse liver. Mice were treated on day 5 after CT26 inoculation with entolimod and livers were collected at the indicated time points for preparation of total protein lysates. IFN-γ levels were measured by ELISA and normalized per μg total protein. Mean ± SEM, $n = 4$ mice per group. *$P < 0.02$ for comparison with 0 h (Student's *t* test). (*B*) Effect of entolimod treatment on expression of CXCL9 and CXCL10 in the livers and plasma of IFN-γ–depleted and nondepleted mice. Mice were treated with rat IgG or anti–IFN-γ antibodies on days 4 and 5 after CT26 inoculation and livers were collected at the indicated time points for preparation of total protein lysates. CXCL9 and CXCL10 levels were measured by ELISA and normalized per μg total protein for liver and per ml plasma. Mean ± SEM, $n = 4$ mice per group. *$P < 0.02$ for comparison with 0 h, #$P < 0.03$ for comparison with rat IgG (Student's *t* test). (*C*) Effect of IFN-γ depletion on entolimod-elicited NK cell response in the liver. Mice were treated with rat IgG or anti–IFN-γ antibodies on days 4 and 5 after CT26 inoculation and livers were collected at the indicated time points for FACS analysis. NK cells were defined as $CD45^+CD3\varepsilon^-NKp46^+$. Results are reported as the absolute number of NK cells per liver. $n = 3$–5 mice per group; *$P < 0.01$ for comparison with control.

Discussion

Recent major breakthroughs in cancer immunotherapy include the development of chimeric antigen receptor therapy (59) and immune checkpoint blockade (60), both of which have reinvigorated the promise of this explosive field of oncologic research. Despite some remarkable successes, however, clinical efficacy has been limited to specific patient populations, such as those with certain B-cell malignancies or advanced melanoma (61). This illustrates the complexities facing the cancer immunotherapy field, but also reaffirms that continued successes may be achieved if development of new treatment paradigms is paired with improved understanding of the biology of different tumor types and relevant antitumor immune mechanisms.

In addition to chimeric antigen receptor therapy and immune checkpoint blockade, considerable interest has been placed on strategies that engage the TLR system, a critical component of host defense that bridges innate and adaptive immunity (7). Although at least nine distinct TLRs have been discovered in mammals (62), drug development efforts have focused on targeting TLRs 3, 7, and 9, because they are thought to effectively integrate innate and adaptive immune responses (63). However, the promise of such TLR agonist-based therapies has not been borne out in the clinic, not only because little attention has been paid to identifying the most suitable target tumor types, but also because systemic administration of the pharmacologics used to engage these particular TLR pathways have led to "cytokine storm"-related dose-limiting toxicities (10–12). This led us to consider that the therapeutic value of the "TLR agonist concept" might be markedly improved by exploiting a TLR system intrinsic to the tumor microenvironment. Based on the knowledge of TLR5 expression in vivo, and the fact that the liver (i.e., hepatocytes) is a dominant sink for the action of TLR5 agonists (26), we hypothesized that liver-associated malignancies would represent rational targets for TLR5-directed immunotherapy.

In agreement with this central hypothesis, earlier studies in our laboratory showed that treatment with the TLR5 agonist entolimod significantly prolonged survival of mice in experimental models of liver metastatic tumors (26). This activity was mediated by an NK cell-dependent mechanism and did not cause cytokine-storm–associated side effects (29). Despite these promising preliminary findings, a number of fundamental questions surrounding the antimetastatic activity of entolimod remain to be resolved, namely: (*i*) Does entolimod treatment prolong survival of tumor-bearing hosts by engaging a combination of both innate and adaptive immune cellular elements, such as NK cells and $CD8^+$ or $CD4^+$ T cells? (*ii*) If the antimetastatic activity of entolimod enhances survival of tumor-bearing hosts through a T-cell–dependent mechanism, does this lead to generation of a memory immune response enabling surviving hosts to reject a subsequent tumor challenge? (*iii*) If both innate and adaptive immune cellular elements are necessary for entolimod-mediated enhancement of survival, what is the dynamic relationship between these two arms of the cell-mediated immune system? (*iv*) How general is the antimetastatic activity of entolimod (e.g., is efficacy observed with other tumor types or other nonliver sites of metastasis)?

Altogether, and in contrast to what has been observed in studies of TLR3 or -9 targeting, our results show that activation of the TLR5 pathway using entolimod as a single-agent systemic monotherapy: (*i*) leads to antimetastatic activity by recruiting and engaging both NK and T-cell responses; (*ii*) enables the generation of $CD8^+$ T-cell–dependent antitumor memory, which

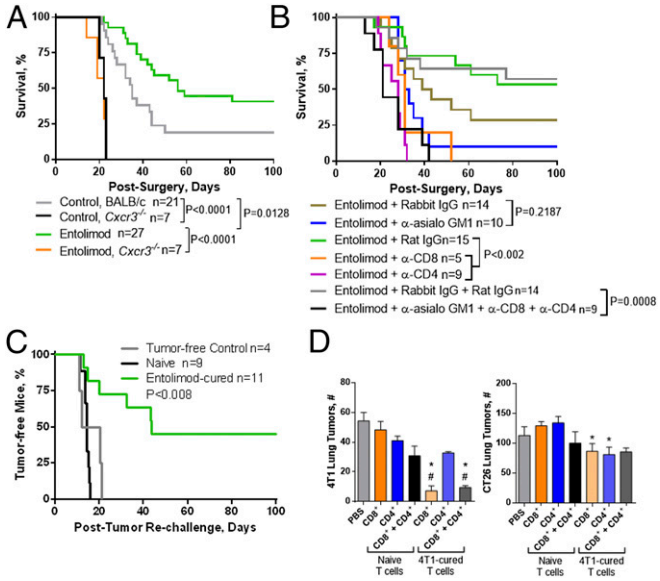

Fig. 4. CXCR3 regulates entolimod-mediated generation of antitumor immunity against spontaneous mammary cancer metastases. (*A* and *B*) Mice were injected (subcutaneously) with PBS (untreated) or entolimod on days 1, 3, and 5 after surgical removal of orthotopic primary 4T1 tumors. *P* values were determined by log-rank test. (*A*) Effect of entolimod treatment on BALB/c and *Cxcr3*$^{-/-}$ animal survival in the 4T1 metastasis model. (*B*) Effect of NK, CD8$^+$, or CD4$^+$ T-cell depletion on survival of entolimod-treated mice in the 4T1 metastasis model. Mice were treated with anti-asialo GM1 (days 0, 1, and 7 postsurgery), anti-CD8 or anti-CD4 (days 0 and 7 postsurgery), or control Abs (rabbit or rat IgG, respectively) in combination with entolimod given on days 1, 3, and 5 postsurgery. (*C*) Entolimod-induced immune memory against 4T1 tumors. Naïve BALB/c mice or entolimod- or PBS (control)-treated mice that survived for >100 d after surgery in the experiment described in *A* were rechallenged with 4T1 tumor cells injected subcutaneously in the opposite mammary fat pad. The percentage of mice showing no development of subcutaneous tumors is plotted over time. *P* values were determined by log-rank test. (*D*) Effect of transferred T cells from mice cured of 4T1 tumors by entolimod treatment or from naïve mice on development of 4T1 or CT26 tumors in the lungs of naïve mice. Naïve BALB/c mice were given an intravenous transfer of naïve or "4T1-cured" T cells (CD4$^+$, CD8$^+$ or CD4$^+$ + CD8$^+$ T cells) 3 d after intravenous injection of 4T1 (*Left*) or CT26 (*Right*) tumor cells. The "PBS" control groups were injected with tumor cells, but did not receive T cells (injected with PBS instead). Mice were killed on day 30 after tumor cell injection and lungs were harvested to quantify the number of lung tumors under a dissecting microscope. Data are shown as mean number of tumors per lung ± SEM (n = 5 mice per group). *P* values were determined by Student's *t* test. $^*P < 0.03$ for comparison with PBS or naïve control, $^{\#}P < 0.003$ for comparison with 4T1-cured CD4$^+$ T cells.

leads to tumor rejection upon rechallenge; (*iii*) suppresses tumor development and metastasis through a mechanism involving CXCR3-dependent homing of NK cells to the liver; and (*iv*) is efficacious against metastasis to the lung as well as the liver for primary tumors of multiple types (demonstrated in murine CT26 CRC and 4T1 mammary tumor models). The overall finding that entolimod treatment as a single-agent can induce long-term antitumor immune control in multiple preclinical models not only suggests that entolimod is likely superior to current TLR-based approaches, but that TLR agonists that engage or hone in on immune reactions within a relevant pathologic microenvironment (such as TLR5 in the liver) are likely to be more effective than those that act systemically or distally from the relevant target site. This organ-specific activity of TLR5-activating agents is supported by recent work demonstrating that T cells capable of secreting bacterial flagellin have enhanced antitumor activity through their ability to reshape the local tumor microenvironment into one that is conducive for an antitumor immune response (64).

Paradoxically, both tumor-promoting inflammation and antitumor immunity have been linked to TLR5. In fact, activation of TLR5 by commensal bacteria was shown to drive malignant progression at extramucosal locations through the promotion of inflammation, which dampened antitumor immunity by expanding immunosuppressive networks (65). In contrast, we and others have shown that TLR5 activation has tumor growth suppressive effects and stimulates antitumor immunity (19–26, 53). Earlier studies in our laboratory showed that entolimod displayed a growth-inhibitory effect on a TLR5-expressing mouse xenograft model of human lung adenocarcinoma A549 (23), supporting a direct effect of TLR5 stimulation on tumor growth suppression. However, our more recent work (26), in conjunction with the work presented here, indicate a second indirect mechanism through TLR5-mediated changes in the liver microenvironment. TLR5 activation in the liver is sufficient for the generation of antitumor immunity, as evident in the TLR5 nonresponsive CT26 liver metastatic model. Hence, TLR5 stimulation suppresses tumor growth and generates antitumor immunity through two mechanisms: (*i*) directly via tumor cells, and (*ii*) indirectly through microenvironmental changes of the liver. The relative impact of these two mechanisms on the generation of antitumor immunity by TLR5 activation is a focus of our future work.

Although immune interactions within the liver in response to TLR5 activation are complex and remain to be fully understood, earlier studies have identified hepatocytes as a direct and major entolimod-responsive cell type in vivo (26). The results presented herein offer new clues into how engagement of this pathway leads to tumor growth control. Fig. 5 illustrates our working model for how entolimod suppresses experimental colorectal liver metastasis by engaging both innate and adaptive immune effector mechanisms. Together with our previous work, this study shows how entolimod stimulates homing of NK cells to naïve (26) and tumor-bearing livers (32). Our data herein show that entolimod-elicited NK cell homing to the liver occurs predominantly through a CXCR3-dependent blood-borne mechanism, but that an alternate mechanism also exists. NK cells have been reported to express multiple chemokine receptors, including CXCR 1–4, CCR4, CCR5, CCR7, CCR8, and CX_3CR1 (66). Because entolimod induces expression of the CXCR1/2 chemokine CXCL1 (29), this chemokine axis may contribute to NK cell homing to the liver. Two other potential candidates are CCL3 (67) and CCR5 (68), both of which control NK cell

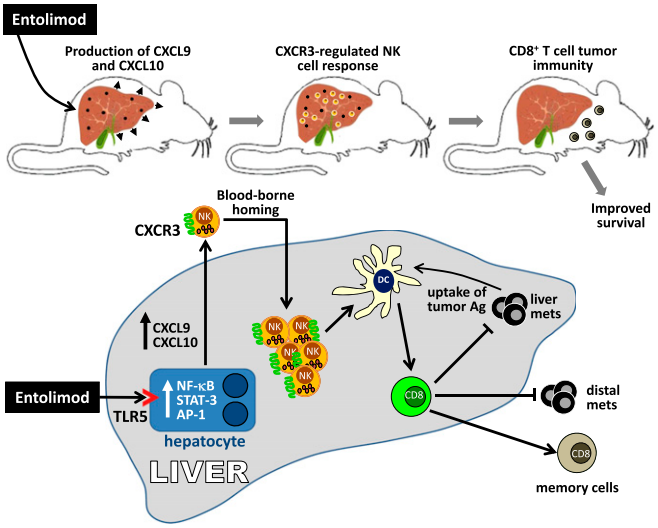

Fig. 5. Schematic illustration of the proposed antimetastatic mechanism of entolimod against experimental colorectal cancer liver metastases.

recruitment to the liver in response to bacterial infection. The coordinated relationship between NK cells and $CD8^+$ T cells leading to optimal therapeutic efficacy of entolimod was demonstrated by subset-specific depletion (loss-of-function) experiments or adoptive transfer (add-back/reconstitution of individual subsets) approaches. Moreover, NK cell depletion studies were used to show that DCs bridged the temporal relationship between NK and $CD8^+$ T cells within the liver tumor microenvironment. Recent work by Riise et al. (69) showing that TLR7-stimulated neutrophils instruct NK cells to stimulate DC maturation may be a potential mechanism for entolimod-mediated NK cell activation of DCs.

In contrast to the CT26 liver metastatic model, suppression of spontaneous mammary metastases in the 4T1 model by entolimod did not absolutely depend upon NK cells, but rather was completely dependent on both $CD8^+$ and $CD4^+$ T cells. An important difference in the metastatic spread of these two models, which may contribute to the difference in the antitumor mechanisms of entolimod, is that the CT26 model produces only liver metastases, whereas the 4T1 model develops both liver and lung metastases. Although the role of $CD4^+$ T cells for the antitumor mechanism of entolimod in the 4T1 model remains unclear, $CD4^+$ T cells potentially provide help for DC activation, costimulatory molecule expression, and production of IL-12 and IFN-γ. A direct interaction of $CD4^+$ T cells with 4T1 tumor cells is unlikely due to the lack of MHC II expression by 4T1 tumor cells (70). The mechanism by which entolimod facilitates the interaction of $CD4^+$ T cells and DCs is unknown and should be a future focus of study.

Although the work of others has shown that NK cells are directly tumoricidal against tumor cells in the liver (36, 37), our findings indicate that NK cells play a regulatory role by stimulating DC activation but not recruitment to the liver post-entolimod. This finding is supported by the current knowledge that NK cells influence T-cell immunity via DC-dependent pathways (as reviewed in ref. 55). Although the mechanism remains unclear, NK cell produced IFN-γ facilitates DC maturation/activation by stimulating increased expression of costimulatory molecules CD86 and CD40 on DCs and production of IL-12 and IFN-γ, all of which are critical for T-cell activation, differentiation, and expansion (71, 72). Similar to other models (42), we identified that entolimod stimulates an NK-DC cross-talk to activate antitumor $CD8^+$ T cells independently of $CD4^+$ T-cell help. Our findings showing that DC activation is not completely abolished in NK cell-depleted mice suggest a minor NK cell-independent mechanism also exists. Entolimod may directly activate liver-specific DCs, which is supported by in vitro studies showing that: (*i*) splenic $CD11c^+$ cells respond directly to entolimod by up-regulation of costimulatory molecules CD80 and CD86 (53), and (*ii*) flagellin directly activates bone marrow DCs in vitro (73) and lamina propria DCs in vivo (74) to drive a Th1 response.

Given the apparent central importance of NK cells as "initiators" of entolimod-mediated antitumor immune responses, we sought to identify the molecular mechanism regulating the entolimod-elicited NK cell response. Induction of the CXCR3 ligand CXCL10 by entolimod in the plasma of treated mice (29) provided the rationale to explore whether this axis regulates the NK cell response induced by entolimod. We demonstrated that abrogation of the NK cell response either by antibody-mediated depletion of NK cells or by disruption of CXCR3-directed NK cell homing (in *Cxcr3*$^{-/-}$ mice) prevented DC activation. This clearly establishes that CXCR3-dependent NK cell homing to the liver after entolimod treatment is required for both DC activation and downstream activation of T-cell–dependent antitumor immunity. Intriguingly, our work shows that entolimod may regulate expression of CXCL9 and CXCL10 through a unique mechanism that is predominantly IFN-γ or IFN-γ signaling-independent. Although the mechanism is unknown, a potential candidate is IFN regulatory factor 1 (IRF-1). Activation of TLRs can directly induce IRF-1 expression (75), which in turn can transcriptionally control expression of the genes for CXCL9, CXCL10, and CXCL11 (76, 77). Moreover, IRF-1 expression was shown to be essential for expression of CXCL11 and suppression of pulmonary metastases by CXCR3-expressing NK cells (78).

In summary, our results demonstrate that entolimod can serve as an effective systemic monotherapy to generate protective antitumor T-cell immunity through coordination with CXCR3-expressing NK cells. Our finding that entolimod mediates antitumor effects in several mouse models, including a model of spontaneous metastasis to distal sites, suggests that entolimod treatment alone or in concert with other conventional or experimental therapies could have a major impact on cancer treatment outcomes. The safety of systemically administered entolimod has been demonstrated in several mammalian species, including rodents, nonhuman primates, and humans (29, 30). Together with this established safety profile, the mechanistic findings of the work reported here provide a strong foundation for initiation of a phase I clinical trial of entolimod in patients with metastatic liver disease to assess its safety as well as its ability to induce innate/adaptive immune responses as surrogate measurements of efficacy (30).

ACKNOWLEDGMENTS. We thank Patricia Baker for her help with the editing of this manuscript; Dr. Joshua Farber for the kind gift of *Cxcr3*$^{-/-}$ mice on the BALB/c background; Liliya Novototskaya for the breeding and maintenance of this colony; and Dr. Xuefang Cao for the samples pertaining to the *Ifngr1*$^{-/-}$ studies. This work was supported by National Institutes of Health Grants R01GM095874 and R01AI080446 (to A.V.G.), and R01CA140622 and R01CA172105 (to S.I.A.); Department of Defense Grant BC140507 (to A.V.G.); a contract from Cleveland BioLabs, Inc. to Roswell Park Cancer Institute (Principal Investigator A.V.G.); and grants from the Roswell Park Alliance Foundation (Principal Investigators S.I.A. and A.V.G.).

1. Restifo NP, Dudley ME, Rosenberg SA (2012) Adoptive immunotherapy for cancer: Harnessing the T cell response. *Nat Rev Immunol* 12(4):269–281.
2. Puré E, Allison JP, Schreiber RD (2005) Breaking down the barriers to cancer immunotherapy. *Nat Immunol* 6(12):1207–1210.
3. Drobits B, et al. (2012) Imiquimod clears tumors in mice independent of adaptive immunity by converting pDCs into tumor-killing effector cells. *J Clin Invest* 122(2): 575–585.
4. O'Sullivan T, et al. (2012) Cancer immunoediting by the innate immune system in the absence of adaptive immunity. *J Exp Med* 209(10):1869–1882.
5. Smyth MJ, et al. (2000) Differential tumor surveillance by natural killer (NK) and NKT cells. *J Exp Med* 191(4):661–668.
6. Kanzler H, Barrat FJ, Hessel EM, Coffman RL (2007) Therapeutic targeting of innate immunity with Toll-like receptor agonists and antagonists. *Nat Med* 13(5):552–559.
7. Akira S, Takeda K, Kaisho T (2001) Toll-like receptors: Critical proteins linking innate and acquired immunity. *Nat Immunol* 2(8):675–680.
8. Rakoff-Nahoum S, Medzhitov R (2009) Toll-like receptors and cancer. *Nat Rev Cancer* 9(1):57–63.
9. Stanley MA (2002) Imiquimod and the imidazoquinolones: Mechanism of action and therapeutic potential. *Clin Exp Dermatol* 27(7):571–577.
10. Adams S, et al. (2008) Immunization of malignant melanoma patients with full-length NY-ESO-1 protein using TLR7 agonist imiquimod as vaccine adjuvant. *J Immunol* 181(1):776–784.
11. Khan AL, Heys SD, Eremin O (1995) Synthetic polyribonucleotides: Current role and potential use in oncological practice. *Eur J Surg Oncol* 21(2):224–227.
12. Manegold C, et al. (2008) Randomized phase II trial of a Toll-like receptor 9 agonist oligodeoxynucleotide, PF-3512676, in combination with first-line taxane plus platinum chemotherapy for advanced-stage non-small-cell lung cancer. *J Clin Oncol* 26(24):3979–3986.
13. Huang B, et al. (2007) Listeria monocytogenes promotes tumor growth via tumor cell toll-like receptor 2 signaling. *Cancer Res* 67(9):4346–4352.
14. Pidgeon GP, et al. (1999) The role of endotoxin/lipopolysaccharide in surgically induced tumour growth in a murine model of metastatic disease. *Br J Cancer* 81(8): 1311–1317.
15. Harmey JH, et al. (2002) Lipopolysaccharide-induced metastatic growth is associated with increased angiogenesis, vascular permeability and tumor cell invasion. *Int J Cancer* 101(5):415–422.
16. Fan H, et al. (2012) Intracerebral CpG immunotherapy with carbon nanotubes abrogates growth of subcutaneous melanomas in mice. *Clin Cancer Res* 18(20):5628–5638.

17. Le Mercier I, et al. (2013) Tumor promotion by intratumoral plasmacytoid dendritic cells is reversed by TLR7 ligand treatment. *Cancer Res* 73(15):4629–4640.
18. Palamara F, et al. (2004) Identification and characterization of pDC-like cells in normal mouse skin and melanomas treated with imiquimod. *J Immunol* 173(5):3051–3061.
19. Sfondrini L, et al. (2006) Antitumor activity of the TLR-5 ligand flagellin in mouse models of cancer. *J Immunol* 176(11):6624–6630.
20. Garaude J, Kent A, van Rooijen N, Blander JM (2012) Simultaneous targeting of Toll- and nod-like receptors induces effective tumor-specific immune responses. *Sci Transl Med* 4(120):120ra16.
21. Cai Z, et al. (2011) Activation of Toll-like receptor 5 on breast cancer cells by flagellin suppresses cell proliferation and tumor growth. *Cancer Res* 71(7):2466–2475.
22. Rhee SH, Im E, Pothoulakis C (2008) Toll-like receptor 5 engagement modulates tumor development and growth in a mouse xenograft model of human colon cancer. *Gastroenterology* 135(2):518–528.
23. Burdelya LG, et al. (2012) Toll-like receptor 5 agonist protects mice from dermatitis and oral mucositis caused by local radiation: Implications for head-and-neck cancer radiotherapy. *Int J Radiat Oncol Biol Phys* 83(1):228–234.
24. Soto LJ, 3rd, et al. (2003) Attenuated *Salmonella typhimurium* prevents the establishment of unresectable hepatic metastases and improves survival in a murine model. *J Pediatr Surg* 38(7):1075–1079.
25. Yam C, et al. (2010) Monotherapy with a tumor-targeting mutant of *S. typhimurium* inhibits liver metastasis in a mouse model of pancreatic cancer. *J Surg Res* 164(2): 248–255.
26. Burdelya LG, et al. (2013) Central role of liver in anticancer and radioprotective activities of Toll-like receptor 5 agonist. *Proc Natl Acad Sci USA* 110(20):E1857–E1866.
27. Carvalho FA, Aitken JD, Gewirtz AT, Vijay-Kumar M (2011) TLR5 activation induces secretory interleukin-1 receptor antagonist (sIL-1Ra) and reduces inflammasome-associated tissue damage. *Mucosal Immunol* 4(1):102–111.
28. Vijay-Kumar M, et al. (2008) Toll-like receptor 5-deficient mice have dysregulated intestinal gene expression and nonspecific resistance to *Salmonella*-induced typhoid-like disease. *Infect Immun* 76(3):1276–1281.
29. Burdelya LG, et al. (2008) An agonist of Toll-like receptor 5 has radioprotective activity in mouse and primate models. *Science* 320(5873):226–230.
30. Adjei A (2011) Entolimod in treating patients with locally advanced or metastatic solid tumors that cannot be removed by surgery. Clinical trial no. NCT01527136. Avaliable at ClinicalTrials.gov. Accessed October 24, 2015.
31. Krivokrysenko VI, et al. (2015) The Toll-like receptor 5 agonist entolimod mitigates lethal acute radiation syndrome in non-human primates. *PLoS One* 10(9):e0135388.
32. Yang H, et al. (2015) The Toll-like receptor 5 agonist entolimod suppresses hepatic metastases in a murine model of ocular melanoma via an NK cell-dependent mechanism. *Oncotarget*, 10.18632/oncotarget.6500.
33. Hossain MS, Ramachandiran S, Gewirtz AT, Waller EK (2014) Recombinant TLR5 agonist CBLB502 promotes NK cell-mediated anti-CMV immunity in mice. *PLoS One* 9(5): e96165.
34. Lise M, Mocellin S, Pilati P, Nitti D (2005) Colorectal liver metastasis: Towards the integration of conventional and molecularly targeted therapeutic approaches. *Front Biosci* 10:3042–3057.
35. Kim S, et al. (2002) In vivo developmental stages in murine natural killer cell maturation. *Nat Immunol* 3(6):523–528.
36. Bahjat KS, et al. (2007) Activation of immature hepatic NK cells as immunotherapy for liver metastatic disease. *J Immunol* 179(11):7376–7384.
37. Dupaul-Chicoine J, et al. (2015) The Nlrp3 inflammasome suppresses colorectal cancer metastatic growth in the liver by promoting natural killer cell tumoricidal activity. *Immunity* 43(4):751–763.
38. Moretta L, et al. (2006) Effector and regulatory events during natural killer-dendritic cell interactions. *Immunol Rev* 214:219–228.
39. Biron CA, Nguyen KB, Pien GC, Cousens LP, Salazar-Mather TP (1999) Natural killer cells in antiviral defense: Function and regulation by innate cytokines. *Annu Rev Immunol* 17:189–220.
40. Gerosa F, et al. (2002) Reciprocal activating interaction between natural killer cells and dendritic cells. *J Exp Med* 195(3):327–333.
41. Mocikat R, et al. (2003) Natural killer cells activated by MHC class I(low) targets prime dendritic cells to induce protective CD8 T cell responses. *Immunity* 19(4):561–569.
42. Adam C, et al. (2005) DC-NK cell cross talk as a novel CD4+ T-cell-independent pathway for antitumor CTL induction. *Blood* 106(1):338–344.
43. Liu X, et al. (2014) Flagellin-induced expression of CXCL10 mediates direct fungal killing and recruitment of NK cells to the cornea in response to *Candida albicans* infection. *Eur J Immunol* 44(9):2667–2679.
44. Luster AD, Ravetch JV (1987) Biochemical characterization of a gamma interferon-inducible cytokine (IP-10). *J Exp Med* 166(4):1084–1097.
45. Loetscher M, et al. (1996) Chemokine receptor specific for IP10 and mig: Structure, function, and expression in activated T-lymphocytes. *J Exp Med* 184(3):963–969.
46. Loetscher M, Loetscher P, Brass N, Meese E, Moser B (1998) Lymphocyte-specific chemokine receptor CXCR3: Regulation, chemokine binding and gene localization. *Eur J Immunol* 28(11):3696–3705.
47. Martín-Fontecha A, et al. (2004) Induced recruitment of NK cells to lymph nodes provides IFN-gamma for T(H)1 priming. *Nat Immunol* 5(12):1260–1265.
48. Wendel M, Galani IE, Suri-Payer E, Cerwenka A (2008) Natural killer cell accumulation in tumors is dependent on IFN-gamma and CXCR3 ligands. *Cancer Res* 68(20):8437–8445.
49. Farber JM (1990) A macrophage mRNA selectively induced by gamma-interferon encodes a member of the platelet factor 4 family of cytokines. *Proc Natl Acad Sci USA* 87(14):5238–5242.
50. Luster AD, Unkeless JC, Ravetch JV (1985) Gamma-interferon transcriptionally regulates an early-response gene containing homology to platelet proteins. *Nature* 315(6021):672–676.
51. Jain A, et al. (2003) Synergistic effect of a granulocyte-macrophage colony-stimulating factor-transduced tumor vaccine and systemic interleukin-2 in the treatment of murine colorectal cancer hepatic metastases. *Ann Surg Oncol* 10(7):810–820.
52. Pulaski BA, Ostrand-Rosenberg S (1998) Reduction of established spontaneous mammary carcinoma metastases following immunotherapy with major histocompatibility complex class II and B7.1 cell-based tumor vaccines. *Cancer Res* 58(7): 1486–1493.
53. Leigh ND, et al. (2014) A flagellin-derived toll-like receptor 5 agonist stimulates cytotoxic lymphocyte-mediated tumor immunity. *PLoS One* 9(1):e85587.
54. Sturge CR, et al. (2013) TLR-independent neutrophil-derived IFN-γ is important for host resistance to intracellular pathogens. *Proc Natl Acad Sci USA* 110(26):10711–10716.
55. Crouse J, Xu HC, Lang PA, Oxenius A (2015) NK cells regulating T cell responses: Mechanisms and outcome. *Trends Immunol* 36(1):49–58.
56. Terabe M, Berzofsky JA (2008) The role of NKT cells in tumor immunity. *Adv Cancer Res* 101:277–348.
57. Jordan MA, Fletcher J, Baxter AG (2004) Genetic control of NKT cell numbers. *Immunol Cell Biol* 82(3):276–284.
58. Ryan MH, Bristol JA, McDuffie E, Abrams SI (2001) Regression of extensive pulmonary metastases in mice by adoptive transfer of antigen-specific CD8(+) CTL reactive against tumor cells expressing a naturally occurring rejection epitope. *J Immunol* 167(8):4286–4292.
59. Barrett DM, Singh N, Porter DL, Grupp SA, June CH (2014) Chimeric antigen receptor therapy for cancer. *Annu Rev Med* 65:333–347.
60. Pardoll DM (2012) The blockade of immune checkpoints in cancer immunotherapy. *Nat Rev Cancer* 12(4):252–264.
61. Hinrichs CS, Rosenberg SA (2014) Exploiting the curative potential of adoptive T-cell therapy for cancer. *Immunol Rev* 257(1):56–71.
62. O'Neill LA, Golenbock D, Bowie AG (2013) The history of Toll-like receptors—Redefining innate immunity. *Nat Rev Immunol* 13(6):453–460.
63. Iwasaki A, Medzhitov R (2004) Toll-like receptor control of the adaptive immune responses. *Nat Immunol* 5(10):987–995.
64. Geng D, et al. (2015) TLR5 ligand-secreting T cells reshape the tumor microenvironment and enhance antitumor activity. *Cancer Res* 75(10):1959–1971.
65. Rutkowski MR, et al. (2015) Microbially driven TLR5-dependent signaling governs distal malignant progression through tumor-promoting inflammation. *Cancer Cell* 27(1):27–40.
66. Maghazachi AA (2003) G protein-coupled receptors in natural killer cells. *J Leukoc Biol* 74(1):16–24.
67. Salazar-Mather TP, Orange JS, Biron CA (1998) Early murine cytomegalovirus (MCMV) infection induces liver natural killer (NK) cell inflammation and protection through macrophage inflammatory protein 1alpha (MIP-1alpha)-dependent pathways. *J Exp Med* 187(1):1–14.
68. Khan IA, et al. (2006) CCR5 is essential for NK cell trafficking and host survival following *Toxoplasma gondii* infection. *PLoS Pathog* 2(6):e49.
69. Riise RE, et al. (2015) TLR-stimulated neutrophils instruct NK cells to trigger dendritic cell maturation and promote adaptive T cell responses. *J Immunol* 195(3):1121–1128.
70. Huang X, et al. (2002) Combined therapy of local and metastatic 4T1 breast tumor in mice using SU6668, an inhibitor of angiogenic receptor tyrosine kinases, and the immunostimulator B7.2-IgG fusion protein. *Cancer Res* 62(20):5727–5735.
71. Yoo JK, Cho JH, Lee SW, Sung YC (2002) IL-12 provides proliferation and survival signals to murine CD4+ T cells through phosphatidylinositol 3-kinase/Akt signaling pathway. *J Immunol* 169(7):3637–3643.
72. Curtsinger JM, Agarwal P, Lins DC, Mescher MF (2012) Autocrine IFN-γ promotes naive CD8 T cell differentiation and synergizes with IFN-α to stimulate strong function. *J Immunol* 189(2):659–668.
73. Vicente-Suarez I, Brayer J, Villagra A, Cheng F, Sotomayor EM (2009) TLR5 ligation by flagellin converts tolerogenic dendritic cells into activating antigen-presenting cells that preferentially induce T-helper 1 responses. *Immunol Lett* 125(2):114–118.
74. Uematsu S, et al. (2008) Regulation of humoral and cellular gut immunity by lamina propria dendritic cells expressing Toll-like receptor 5. *Nat Immunol* 9(7):769–776.
75. Honda K, Taniguchi T (2006) IRFs: Master regulators of signalling by Toll-like receptors and cytosolic pattern-recognition receptors. *Nat Rev Immunol* 6(9):644–658.
76. Kanda N, Shimizu T, Tada Y, Watanabe S (2007) IL-18 enhances IFN-gamma-induced production of CXCL9, CXCL10, and CXCL11 in human keratinocytes. *Eur J Immunol* 37(2):338–350.
77. Harikumar KB, et al. (2014) K63-linked polyubiquitination of transcription factor IRF1 is essential for IL-1-induced production of chemokines CXCL10 and CCL5. *Nat Immunol* 15(3):231–238.
78. Ksienzyk A, et al. (2011) IRF-1 expression is essential for natural killer cells to suppress metastasis. *Cancer Res* 71(20):6410–6418.